Supporting Information

Effect of Molecular Crowding on the Stability of RNA G-Quadruplexes with Various Numbers of Quartets and Lengths of Loops

Saki Matsumoto[a], Hisae Tateishi-Karimata[a], Shuntaro Takahashi[a], Tatsuya Ohyama[a], Naoki Sugimoto[a, b, *]

[a] Frontier Institute for Biomolecular Engineering Research (FIBER), Konan University, 7-1-20 Minatojima-Minamimachi, Kobe 650-0047, Japan.

[b] Graduate School of Frontiers of Innovative Research in Science and Technology (FIRST), Konan University, 7-1-20 Minatojima-Minamimachi, Kobe 650-0047, Japan.

* To whom correspondence should be addressed. Tel: (+81)78-303-1416; Fax: (+81)78-303-1495; Email: sugimoto@konan-u.ac.jp

Contents:

Figure S1. CD spectra of G_mU_n.

Figure S2. Native polyacrylamide gel electrophoresis (PAGE) of G_mU_n.

Figure S3. Plot of T_m values versus ln[G_3U_3].

Figure S4. UV melting curves for 5 μM of G_mU_n.

Figure S5. Plots of ln K_{obs} versus ln a_w for G_mU_n.

Figure S6. UV melting curves for 5 μM of G_2U_3, G_2U_4, G_2U_{171}, and G_2U_{252}.

Table S1. ΔH^o and $T\Delta S^o$ values of G_mU_n in molecular crowding conditions.

Table S2. The melting temperatures (T_m) of G_mU_3 in 20 wt % PEG8000.

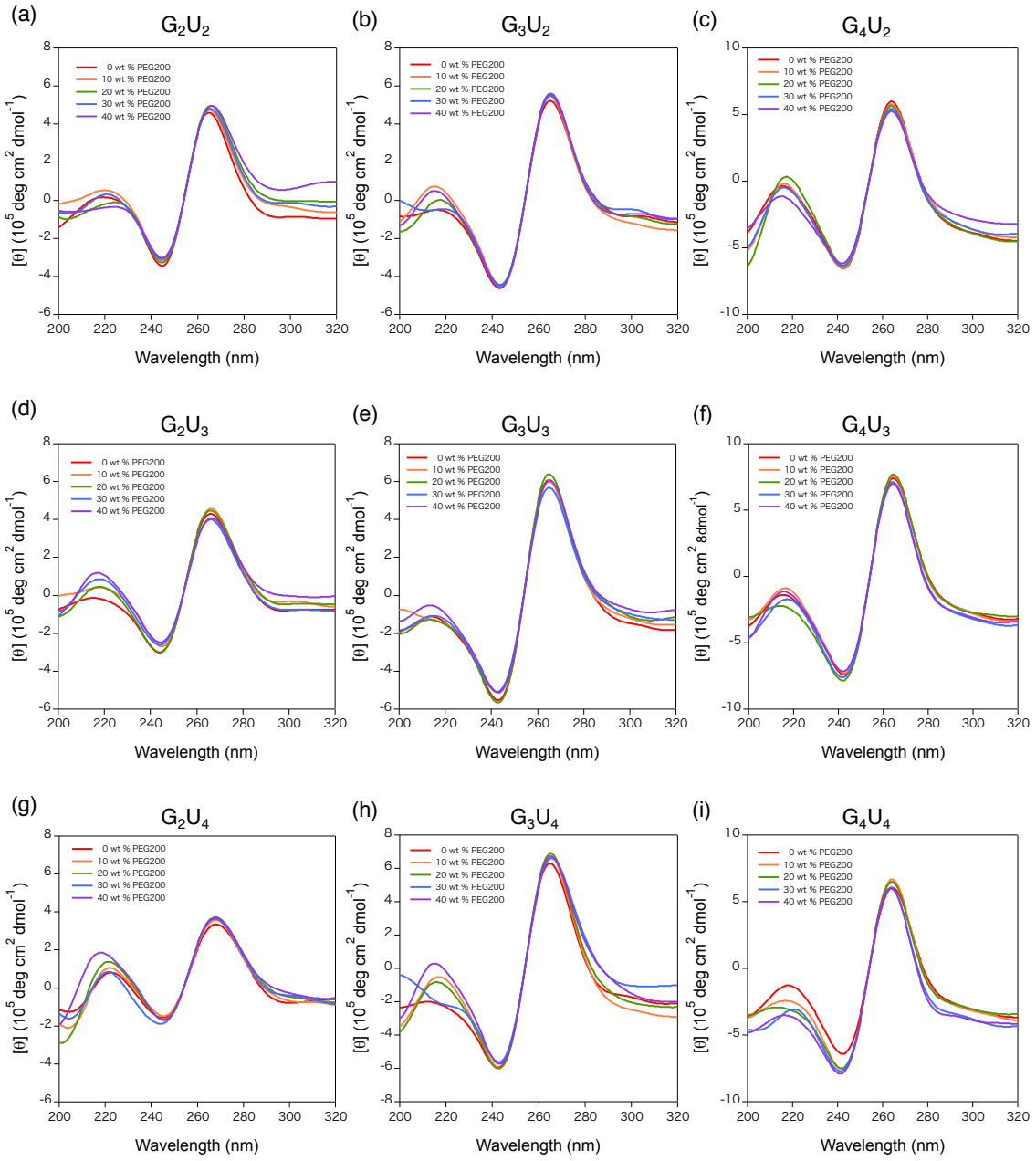

Figure S1. CD spectra for (a) G_2U_2, (b) G_3U_2, (c) G_4U_2, (d) G_2U_3, (e) G_3U_3, (f) G_4U_3, (g) G_2U_4, (h) G_3U_4, and (i) G_4U_4. All experiments were carried out at 4 ºC in 50 mM MES-LiOH (pH 7.0) and 3 mM KCl containing 0－40 wt% PEG200 as indicated: red for 0 wt % PEG200, orange for 10 wt % PEG200, green for 20 wt % PEG200, blue for 30 wt % PEG200, and purple for 40 wt % PEG200.

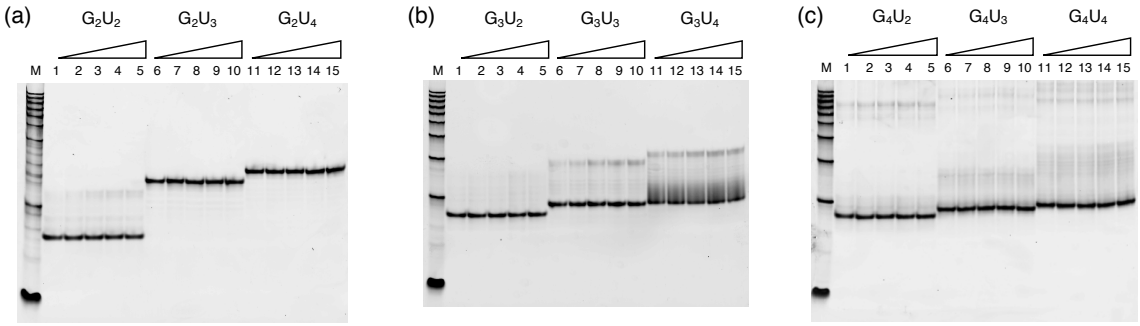

Figure S2. Nondenaturing gel electrophoresis of (a) G_2U_n (n = 2, 3, or 4), (b) G_3U_n (n = 2, 3, or 4), and (c) G_4U_n (n = 2, 3, or 4) at 4 ºC in the buffer containing 3 mM KCl and 50 mM MES-LiOH (pH 7.0) with 0 − 40 wt % of PEG200. Lane M: 10 bp DNA standard; Lanes 1, 6, and 11; without PEG200: lanes 2, 7, and 12; with 10 wt % PEG200: lanes 3, 8, and 13; with 20 wt % PEG200: lanes 4, 9, and 14; with 30 wt % PEG200: lanes 5, 10, and 15; with 40 wt % PEG200.

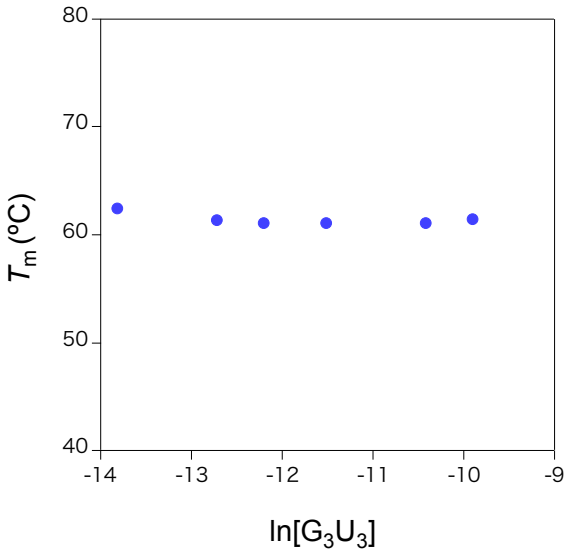

Figure S3. Plot of T_m values versus ln[G_3U_3] strand concentration (1 − 50 μM) in 50 mM MES-LiOH (pH 7.0) containing 3 mM KCl.

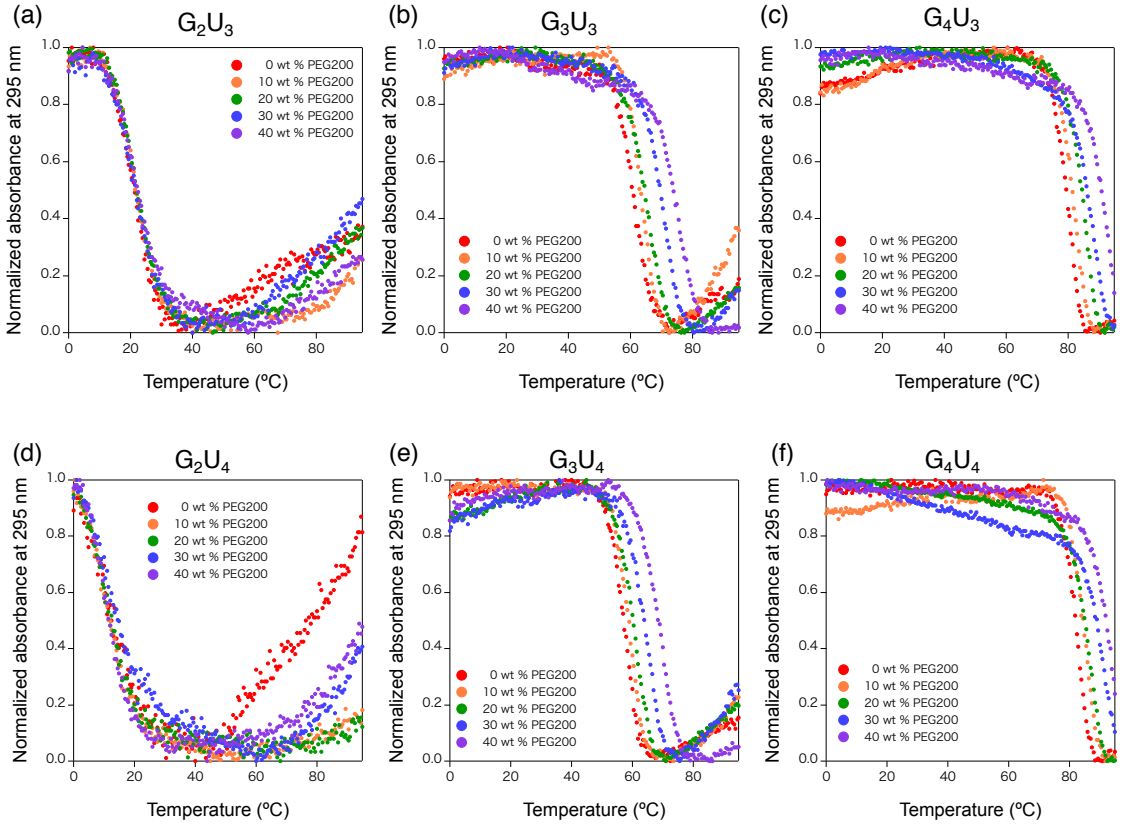

Figure S4. UV melting curves for 5 μM (a) G_2U_3, (b) G_3U_3, (c) G_4U_3, (d) G_2U_4, (e) G_3U_4, and (f) G_4U_4. The melting profiles were determined in 50 mM MES-LiOH (pH 7.0) and 3 mM KCl containing 0－40 wt % PEG200 as indicated: red for 0 wt % PEG200, orange for 10 wt % PEG200, green for 20 wt % PEG200, blue for 30 wt % PEG200, and purple for 40 wt % PEG200.

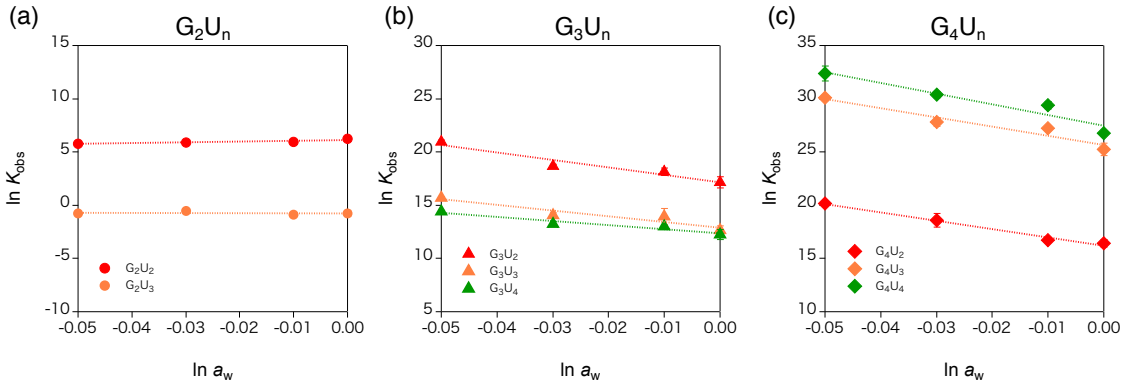

Figure S5. Plots of ln K_{obs} versus ln a_w for (a) G_2U_2 (red) and G_2U_3 (orange), (b) G_3U_2 (red), G_3U_3 (orange), and G_3U_4 (green) (c) G_4U_2 (red), G_4U_3 (orange), and G_4U_4 (green) in 50 mM MES-LiOH (pH 7.0) and 3 mM KCl containing 0－40 wt % PEG200 at 25 ºC.

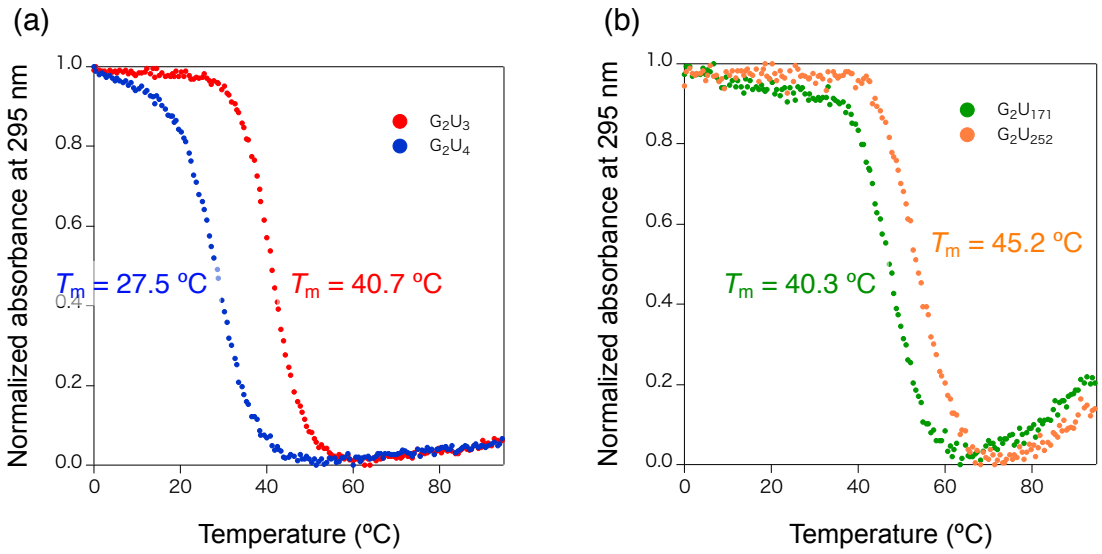

Figure S6. UV melting curves for 5 μM of (a) G_2U_3 (red) and G_2U_4 (blue), and (b) G_2U_{171} (green) and G_2U_{252} (orange). The melting profiles were determined in 50 mM MES-LiOH (pH 7.0) and 140 mM KCl containing 40 wt % PEG200.

Table S1. ΔH^{o} and $T\Delta S^{o}$ values of G_mU_n in molecular crowding conditions[a]

PEG200	0 wt %		10 wt %		20 wt %		30 wt %		40 wt %	
	ΔH^{o} [b]	$T\Delta S^{o}$ [c]	ΔH^{o} [b]	$T\Delta S^{o}$ [c]	ΔH^{o} [b]	$T\Delta S^{o}$ [c]	ΔH^{o} [b]	$T\Delta S^{o}$ [c]	ΔH^{o} [b]	$T\Delta S^{o}$ [c]
G_2U_2	–58.0 ± 2.1	–54.3 ± 2.0	–56.4 ± 1.8	–52.9 ± 1.8	–58.6 ± 1.9	–55.1 ± 1.8	–55.7 ± 0.7	–52.3 ± 0.7	–56.6 ± 0.9	–53.0 ± 0.9
G_3U_2	–74.6 ± 1.2	–64.4 ± 1.5	–75.0 ± 0.3	–64.3 ± 0.1	–75.6 ± 0.5	–64.5 ± 0.4	–78.7 ± 0.8	–66.3 ± 0.7	–80.0 ± 1.0	–66.6 ± 0.9
G_4U_2	–72.4 ± 0.6	–62.7 ± 0.4	–72.9 ± 0.8	–63.0 ± 0.7	–74.6 ± 0.2	–63.6 ± 0.2	–75.3 ± 0.5	–63.3 ± 0.5	–76.3 ± 0.4	–63.5 ± 0.3
G_2U_3	–43.8 ± 1.8	–44.2 ± 1.9	–46.1 ± 0.7	–46.6 ± 0.7	–44.1 ± 1.1	–44.4 ± 1.1	–42.9 ± 2.3	–43.3 ± 2.3	–45.1 ± 1.4	–45.5 ± 1.5
G_3U_3	–69.5 ± 1.8	–62.0 ± 1.6	–70.5 ± 1.2	–62.3 ± 0.8	–70.9 ± 0.2	–62.5 ± 0.3	–71.8 ± 0.5	–62.5 ± 0.4	–73.1 ± 0.7	–62.8 ± 0.6
G_4U_3	–97.9 ± 0.9	–82.9 ± 0.6	–102.3 ± 0.3	–86.1 ± 0.3	–103.1 ± 1.5	–86.6 ± 1.3	–104.7 ± 0.6	–86.8 ± 0.5	–105.2 ± 0.9	–86.2± 0.7
G_2U_4	ND[d]	ND[d]	ND[d]	ND[d]	ND[d]	ND[d]	ND[d]	ND[d]	ND[d]	ND[d]
G_3U_4	–73.3 ± 0.5	–66.0 ± 0.3	–74.0± 1.6	–66.3 ± 1.6	–74.3 ± 0.7	–66.4 ± 0.6	–74.7 ± 0.4	–66.1 ± 0.3	–75.2 ± 0.2	–65.9 ± 0.1
G_4U_4	–100.6 ± 0.7	–84.7 ± 0.6	–104.7 ± 1.2	–87.6 ± 0.8	–106.4 ± 1.1	–88.6 ± 1.0	–108.4 ± 1.4	–89.5 ± 1.1	–109.7 ± 1.3	–89.9 ± 0.8

[a]The values were determined in 50 mM MES-LiOH (pH 7.0) and 3 mM KCl containing different concentrations of PEG200. Each value is the average of three determinations along with the standard deviation. [b]ΔH^{o} (kcal mol^{-1}) [c]$T\Delta S^{o}$ (kcal mol^{-1}) [d]Values could not be obtained from the melting curves.

Table S2. Melting temperatures (T_m) of G_mU_3 in 20 wt % PEG8000 [a]

	T_m (ºC)
G_2U_3	23.6 ± 0.2
G_3U_3	67.7 ± 0.7
G_4U_3	82.9 ± 0.5

[a]The values were determined in 50 mM MES-LiOH (pH 7.0) and 3 mM KCl containing 20 wt % PEG8000. Each value is the average of three determinations along with the standard deviation.